

Influence of mechanical milling on microstructure of 49Fe-49Co-2V soft magnetic alloy

J. HE, F. ZHOU

Department of Chemical and Biochemical Engineering and Materials Science,
University of California Irvine, Irvine, CA 92697-2575, USA

G. CHANG

Printronic Inc., 14600 Myford Road, Irvine, CA 92623, USA

E. J. LAVERNIA

Department of Chemical and Biochemical Engineering and Materials Science,
University of California Irvine, Irvine, CA 92697-2575, USA

E-mail: lavernia@uci.edu

49Fe-49Co-2V pre-alloyed powder was mechanically milled in Methanol for 60 hours. The morphology and microstructure of the as-received and milled powders were characterized by scanning electron microscopy, X-ray diffraction, transmission electron microscopy and thermal analysis. Plastic deformation of about 440% was achieved in the powders milled for 60 hours. The average grain size was found to be 35 nm after milling of 20 hours and it kept essentially constant on further milling up to 60 hours. On the basis of the observations of particle size and morphology, it is suggested that the mixing, caused by overlapping, cold welding and fracturing among particles, did not play an important role in the milling of 49Fe-49Co-2V powder. No new phases were formed during milling process, however, milling enhanced the 550°C anomaly. © 2001 Kluwer Academic Publishers

1. Introduction

The Fe-Co family of alloys often exhibits a high saturation magnetization and Curie temperature, particularly those alloys with chemical compositions of 25 to 50 wt.% Co [1, 2].

The Fe-Co phase diagram is shown in Fig. 1 [3]. The alloys in the composition ranging from 26 to 72 wt.% Co experience an ordered (α' -CsCl structure) \leftrightarrow disordered (α -bcc) phase transformation. The maximum order \leftrightarrow disorder transition temperature of 730°C occurs at the composition of 49 wt.% Co (equiatomic composition). The temperatures of the α (bcc) \leftrightarrow γ (fcc) and magnetization transformations are also observed to be Co composition dependent. The maximum Curie temperature and the maximum $\alpha \leftrightarrow \gamma$ transition temperature appear with a composition of 46 wt.% Co.

In addition to the phase transformations illustrated in the phase diagram, many works have reported a so-called 550°C anomaly in Fe-Co alloys [2, 4, 5]. Discontinuities in the specific heat, temperature dependence of the electrical resistance, saturation magnetization and thermo-electromotive forces have been observed around 550°C [2, 4, 5]. This 550°C anomaly was considered to be related to the presence of a metastable disordered Fe-Co phase because of the absence of the 550°C anomaly in the equilibrium structure [5]. Turgut *et al.* [2], however, observed the 550°C anomaly in high diffusivity nanocrystalline systems which quickly reach

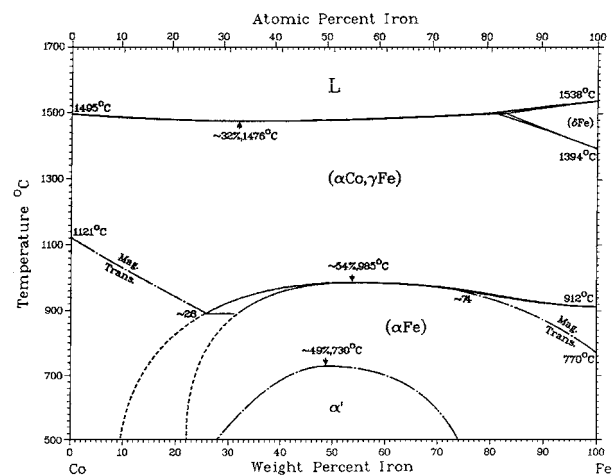


Figure 1 Fe-Co binary alloy phase diagram [3].

equilibrium at relatively low temperatures and argued that the results support an earlier suggestion made by Goman'Kov *et al.* [6]. This suggestion proposed that the 550°C anomaly is due to the difference in partial magnetic moments at temperatures above the anomaly temperature.

Significant interest, including the improvement of magnetic properties, has been generated recently in the field of nanocrystalline materials [7]. Nanocrystalline Fe-based soft magnetic alloys prepared by annealing melt-spun amorphous precursors are one of the most

significant developments in the field of soft magnetic alloy [8]. High soft-magnetic behavior is attributed to the reduced effects of the intrinsic magnetocrystalline anisotropy by reducing the grain size to less than the exchange correlation length [9]. In the nanocrystalline Fe-Co powders synthesized by a rf plasma torch [2] and a carbon-arc [10], the properties of the alloys have been significantly changed. Grain refinement is the most important approach to decrease the brittleness, which limits the application of the 49Fe-49Co-2V alloy [11]. Mechanical alloying/milling techniques have been used to produce large quantities of nanocrystalline materials for possible commercial use [7]. However, few studies on the formation of nanocrystalline 49Fe-49Co-2V by mechanical milling have been reported. In this work, atomized 49Fe-49Co-2V alloy powders are mechanically milled in methanol for various times with the aim to synthesize nanostructure in this alloy. The morphological change and the microstructural evolution on the milling process are characterized in detail and the influence of the milling on phase transformations in the alloy is also addressed.

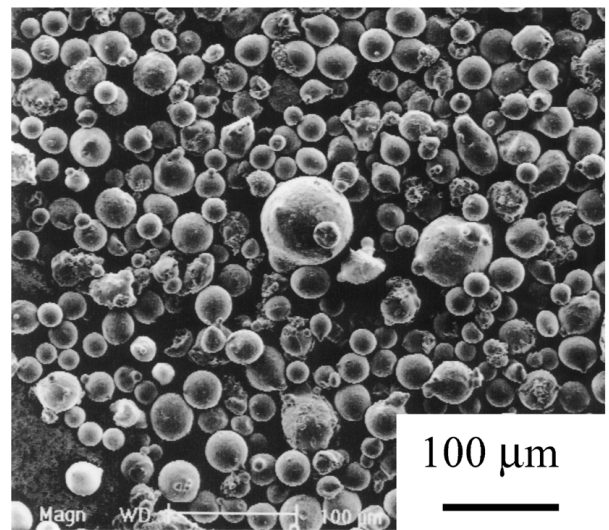
2. Experimental procedure

Commercially available 49Fe-49Co-2V pre-alloyed powder (UltraFine Powder Technology, Inc.) with a nominal powder size of (15–44) microns was used for this study. The powder was immersed in Methanol, and then mechanically milled in a stainless steel tank with stainless steel balls using a 01-HD Union Process attritor at a rate of 250 rpm. The ball to powder mass ratio was 20:1. The milling time was 60 hours. At pre-determined intervals during the milling process, small amounts of powder were removed to follow the microstructural evolution. Scanning electron microscopy (SEM) analysis was performed on a Philips XL 30 FEG microscope. X-ray diffraction (XRD) measurements were carried out using a Siemens D5000 diffractometer equipped with a graphite monochromator using Mo $K\alpha$ ($\lambda = 0.070923$ nm) radiation scans with a step-size of 0.01° and step-time of 5s. Transmission electron microscopy (TEM) observations were conducted using a Philips CM 20 microscope operated at 200 keV. The chemical analysis of the as-received and milled powders was conducted, on the basis of ASTM E 1019 and ASTM E1097 standards, by Luvak Inc., a professional chemical analysis company located in Boylston, Massachusetts. Thermal analysis experiments for the as-received and milled powders were conducted using Perkin-Elmer DTA7 differential thermal analyzer (DTA) and DSC7 differential scanning calorimeter (DSC).

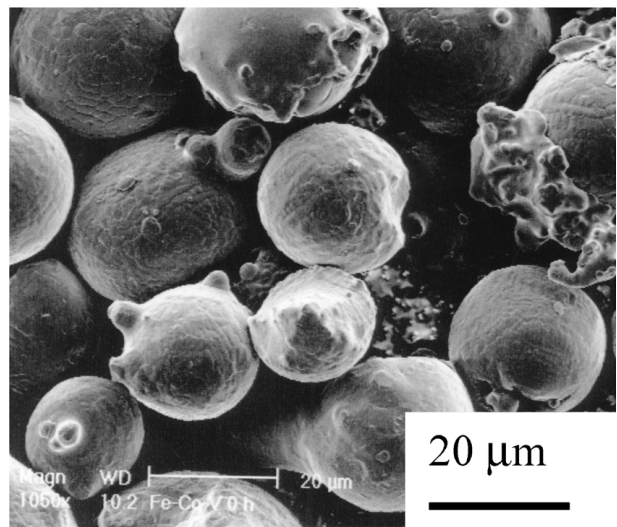
3. Results and discussion

3.1. Changes of morphology and particle size of powders on milling

The as-received powder consisted of spherical particles, most of which contained surface fragments, as shown in Fig. 2. The fragments may be attributed to droplet-droplet impact and satellite formation during



(a)



(b)

Figure 2 Morphology of the as-received 49Fe-49Co-2V powder. (a) The as-received powder; (b) Magnification of (a).

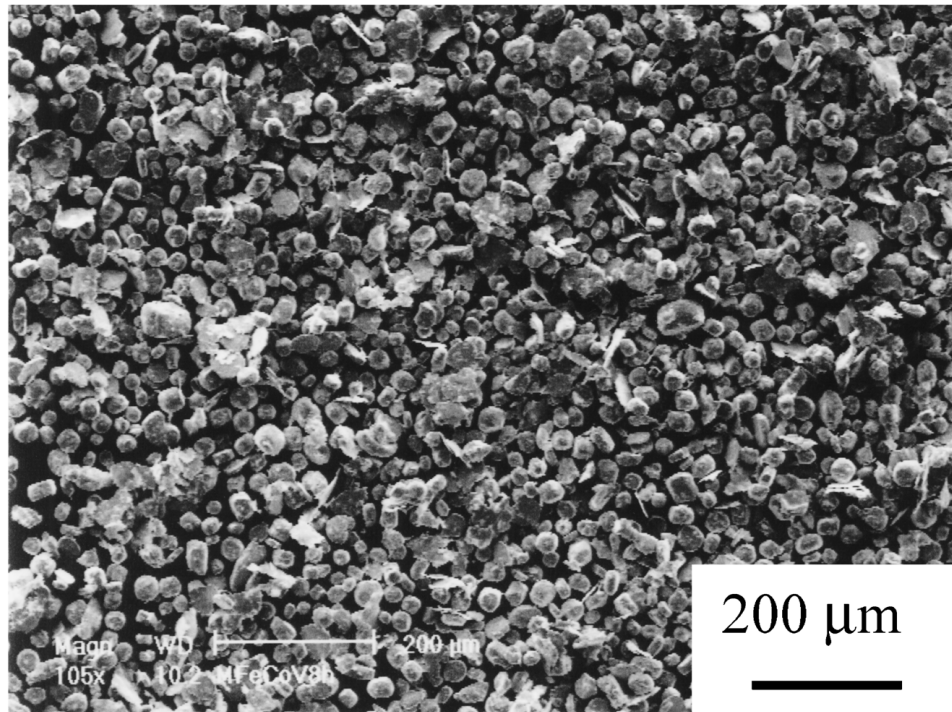
atomization. Fig. 3a–c reveal the morphology of the powders milled for 8, 20 and 48 hours, respectively. After milling for 8 hours, some spherical particles are still observed. The spherical particles gradually change to a flat disk-like morphology as milling time increases. All the particles were found to be disk-like in shape after milled for 36 hours. The diameter and thickness of the disks are statistically measured and plotted in Fig. 4. As milling time increases, the particle diameter increases and the thickness decreases. Maximum plastic deformation is approximately 440% (d/d_0 is nearly equal to 4.4, where d_0 is the average diameter of the as-received powder, d is the average diameter of the powder milled for 60 hours). It is interesting to note that the average volume of the particles remains nearly constant at around $7100 \mu\text{m}^3$ throughout the milling process. Fig. 5 shows a detailed view of the milled powder. The disk-like particles have a morphology that is uniform throughout. In previous studies on other materials [13–16], the agglomerated particles usually have a non-uniform morphology. Examination of statistics of particle size and morphology indicates

that the mixing caused by overlapping, cold welding and fracturing, among particles may not be noticeable although this process does occur occasionally. There are many fine fragments on the surfaces of the particles, which were not counted while measuring the diameter and thickness of the particles. The density of the fine fragments increases with increasing milling time. Fig. 6 shows surface detailed views of the particles. There are a few nanometer-sized fragments and deformed regions with a concave morphology on the surface of the particles that were subjected to 8 hours of milling. A

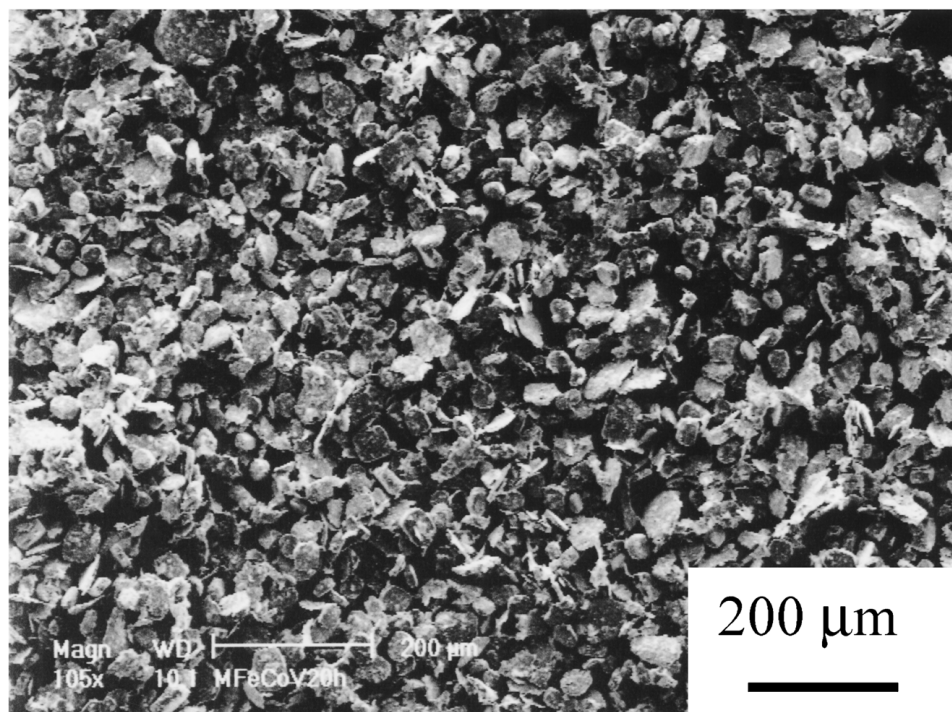
high density of fine fragments is found to agglomerate while deformed regions with a concave morphology were observed on the surface of the particles milled for 48 hours. These two characteristics found on the surfaces of the particles are thought to impede particle mixing.

3.2. The Change of chemical composition on milling

Chemical compositions of the as-received and the 48 hour milled powders are listed in Table I.



(a)

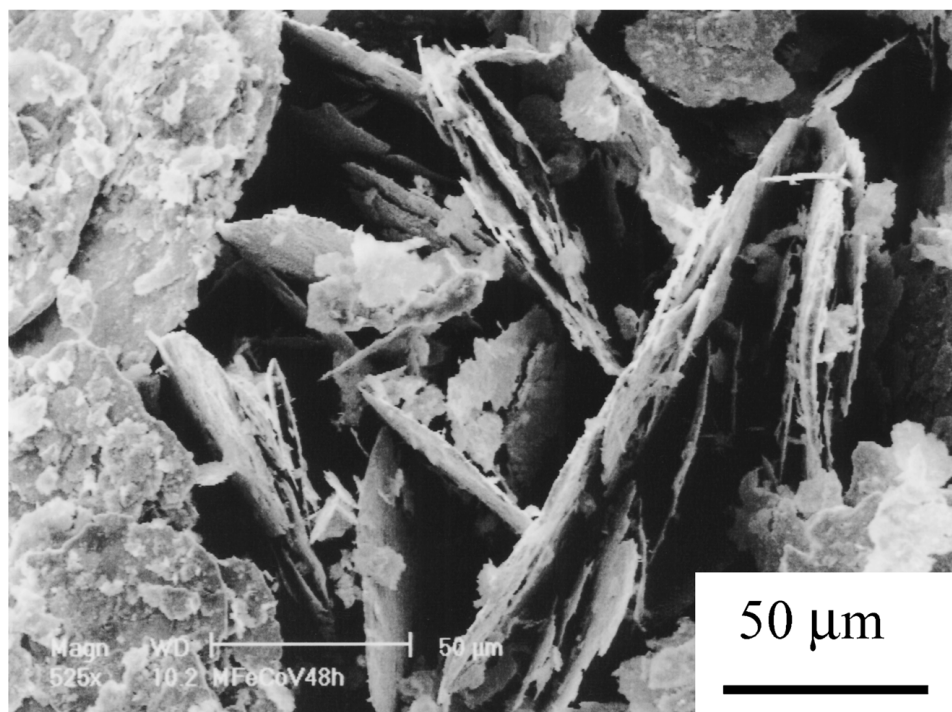


(b)

Figure 3 Morphology of the milled 49Fe-49Co-2V powders. (a) The powder milled for 8 hours; (b) The powder milled for 20 hours; (c) The powder milled for 48 hours; and (d) Magnification of (c). (Continued.)



(c)



(d)

Figure 3 (Continued).

TABLE I Chemical compositions of the as-received and 48 hour milled powders

	Fe	Co	V	Ni	Cr	C	N	O
As-received	49.8	46.8	2.34	0.38	0.20	0.085	0.01	0.028
48 h milled	48.0	43.3	2.21	0.40	0.24	0.613	0.057	4.17
48 milled*	50.08	45.18	2.31	0.42	0.24	0.622	0.058	—

*Chemical composition, excluding oxygen, of the powder milled for 48 hours.

The milling has not noticeably changed the amount of Fe, Co, V, Ni and Cr. This indicates that the stainless tools (vessel, shaft and balls) have not introduced excess impurities into the powders. However, the amount of C, N and O has increased significantly, probably as a result of the Methanol environment. It was found that, in a related study on Fe-Co alloy, the change in Co content from 39 to 49% did not markedly affect the temperature of disorder-order transformation [17].

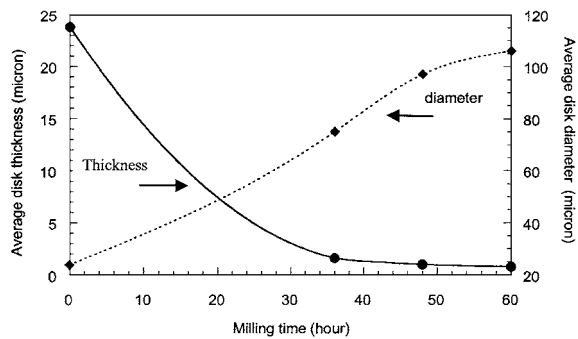
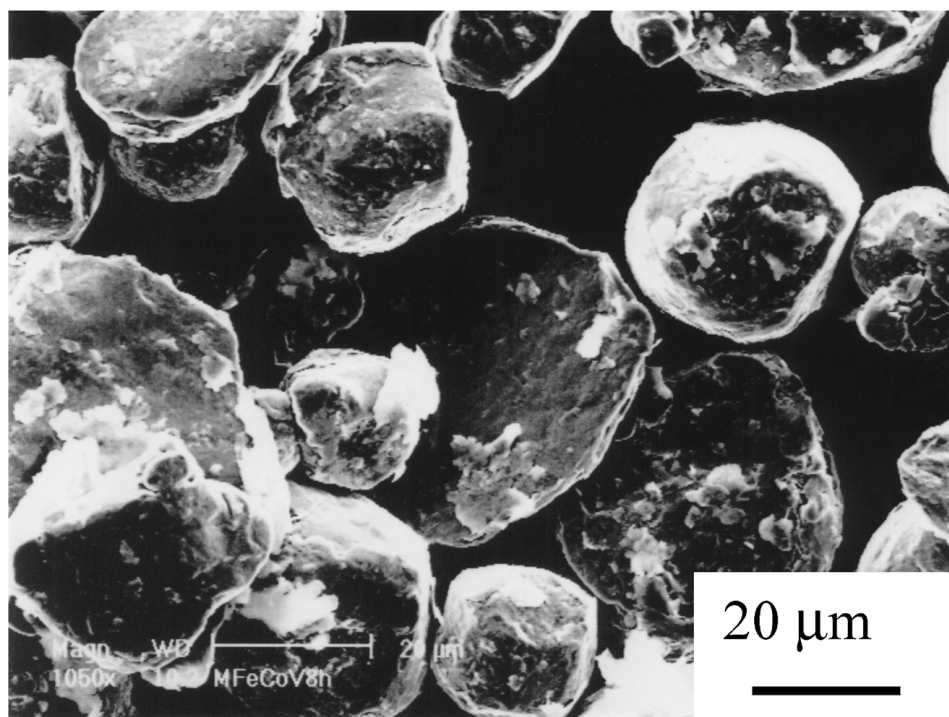
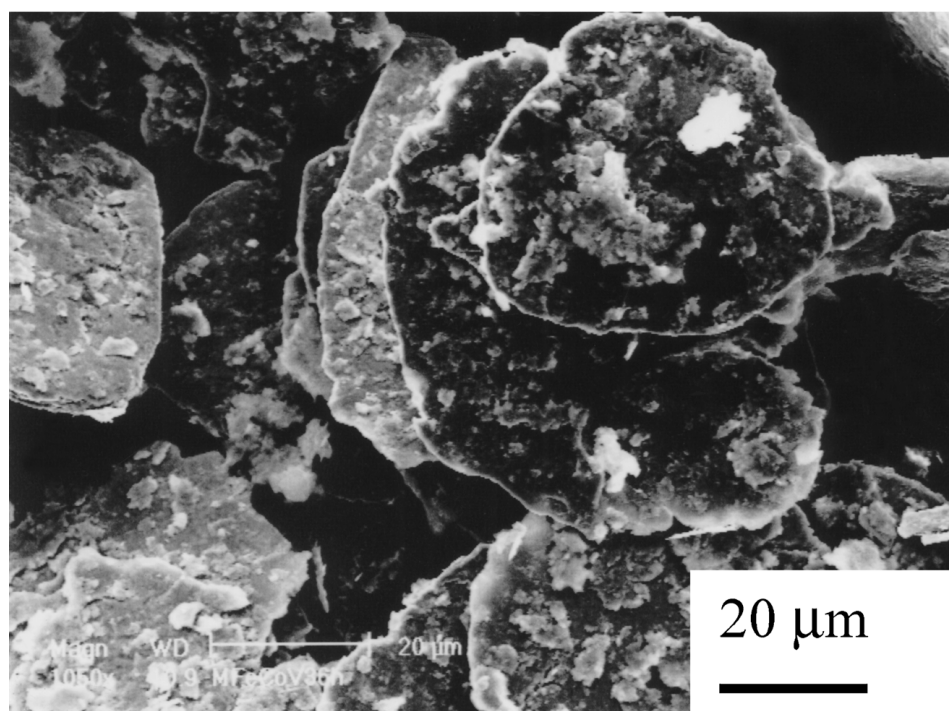


Figure 4 Variation of disk powder size with milling time.

Thermal expansion measurements did reveal that an increase in Ni content in the range of 0–1 wt.% decreased the $\alpha \rightarrow \gamma$ transformation temperature slightly, the effect of increasing Ni depressing the $\alpha \rightarrow \gamma$ transformation temperature is similar to that when V content was increased [18]. The addition of 3–8% Ni has beneficial effects on the ductility and strength without serious degradation of the magnetic properties [19]. In case of the presence of a large amount of C, the influence on phase transformation has not been reported [10]. The information on the possible influence of O and N on phase transformations is not available. The mechanical

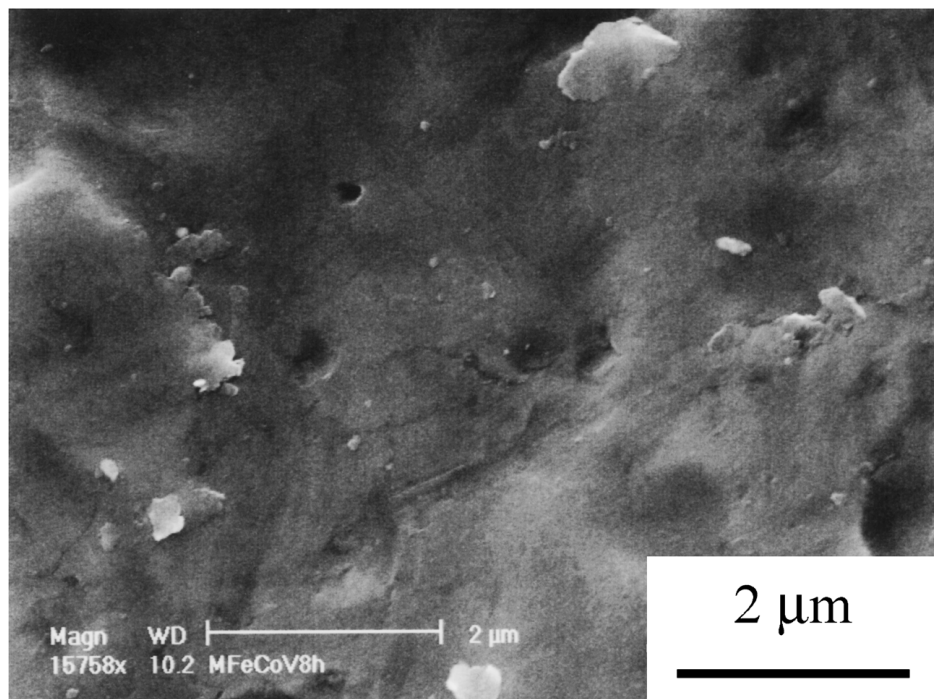


(a)

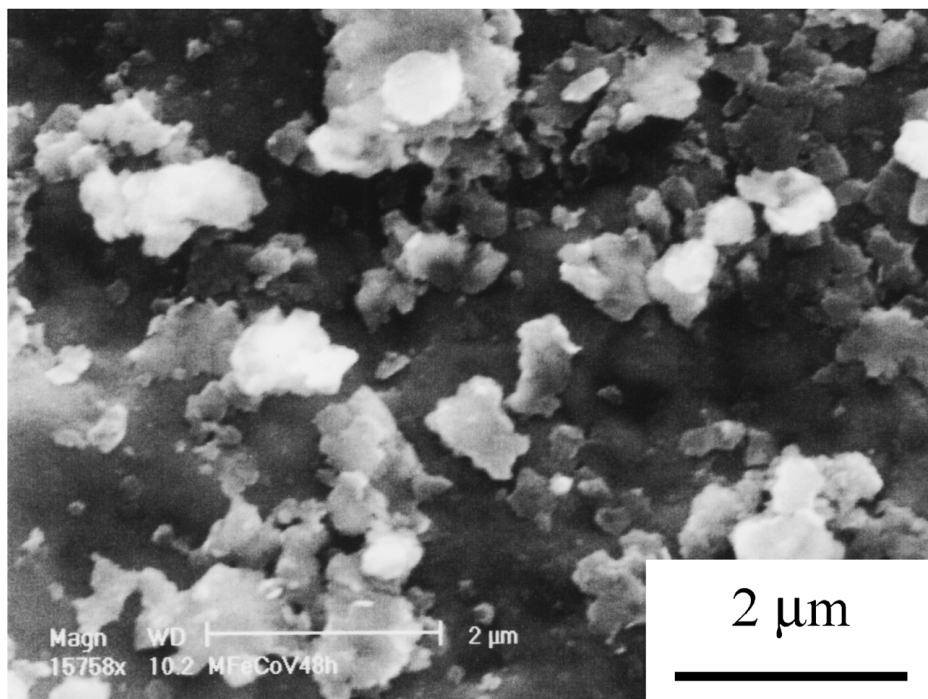


(b)

Figure 5 Top views of the milled 49Fe-49Co-2V powders. (a) The powder milled for 8 hours; (b) The powder milled for 36 hours.



(a)



(b)

Figure 6 Fine fragments and concave deformed traces on the surface of the milled 49Fe-49Co-2V powders. (a) The powder milled for 8 hours; (b) The powder milled for 48 hours.

and magnetic properties are sensitive to the purity of the alloy [11]. The chemical composition dependence of phase transformations is complex and outside of the scope of the present study. The present work considers “milling conditions (stainless tools, milling media and dynamics)” as complex factors, and then discusses the influence of milling time.

3.3. Structural evolution on the milled powders

The XRD spectra of the as-received and milled powders are shown in Fig. 7. Only the diffraction peaks of α -Fe

are observed in these samples though it was reported that the alloy consist of multi-phases [17–19]. The additions of Co and V do not lead to the formation of new XRD peaks. The XRD peaks from the ordered phase α' cannot be observed as a result of their low intensity; This can be attributed to the similarity in atomic scattering factors of Fe and Co. For the α' -CsCl structure, the atomic scattering factor (F_{hkl}) is equal to $(f_{Fe} + f_{Co})$ in the positions of $h + k + l = \text{even}$; and $(f_{Fe} - f_{Co})$ in the positions of $h + k + l = \text{odd}$, this correlates with where the superlattice reflection peaks of the ordered phase should appear. However, f_{Fe} is nearly equal to f_{Co} [20], and hence F_{hkl} approaches zero when $h + k + l = \text{odd}$.

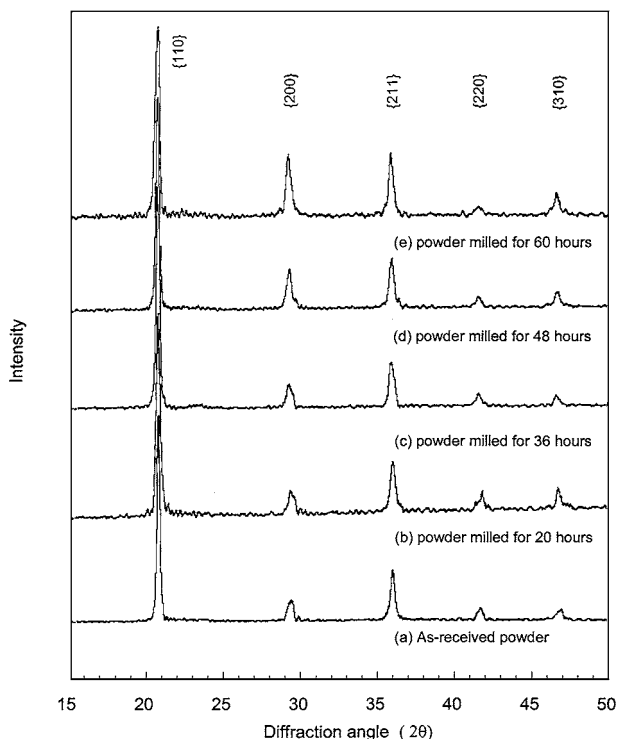


Figure 7 X-ray diffraction spectra of 49Fe-49Co-2V powders milled for different times.

Thus, diffraction peaks from the ordered phase cannot be observed. There are no new peaks in the XRD spectra of the milled powders. As milling time increases up to 20 hours, XRD peaks became broadening, however, a further change in magnitude of peak broadening is not observed after the milling time is over 20 hours although plastic deformation continuously increase up to approximately 440%. This may be due to the absence of particle reconstruction caused by mixing during the milling process.

The average grain size and the strain of the milled powders, following different milling times, were determined using Equation 1 [21]:

$$\beta \cos \theta = 2\varepsilon \sin \theta + 0.9\lambda/D \quad (1)$$

where β is the pure broadening of the diffraction peak measured at half the maximum intensity, θ is the Bragg angle, ε is the average strain, λ is the wavelength of the X-ray radiation (in the present study, $\lambda = 0.07092$ nm), and D is the average dimension of crystallites. The calculated results are plotted in Fig. 8. The average grain size is decreased down to approximately 33 ± 4 nm in the powders milled for 20 hours. At longer milling times, the average grain size keeps essentially constant. The average strain is found to be about 0.5% in the sample milled for 20 hours. With an increase of milling time, it increases slightly, being a maximum value of approximately 0.7% at 48 hour milling and a value of 0.6% in the final status.

The TEM observations confirm the XRD results. A network-like structure is observed in the as-received powder, as shown in Fig. 9a. Fig. 9a–d show bright images of the powders milled for 20 hours, 48 hours, and 60 hours, respectively. The network-like structure

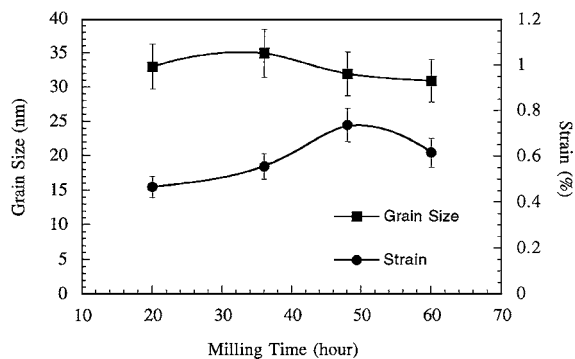


Figure 8 Variation of average grain size and strain in the 49Fe-49Co-2V sample with milling time.

is extensively observed. As milling time increases, the network-like structure is fractured into arcs shapes as shown in the powder milled for 48 hours, and then fractured into particles with an average size of approximately 30 nm, as shown in the powder milled for 60 hours. Apparently, only {110}, {200}, {211}, {220} and {310} diffraction rings of α -Fe are identified, consistent with our XRD measurement results. The superlattice diffraction patterns from the ordered α' phase cannot be observed in the electron diffraction pattern due to the similar atomic scattering factors of Fe and Co. Diffraction patterns from martensite are also not observed because of the same crystal structure and lattice parameters of the α phase [11]. Thus it is impossible to obtain a dark field image of an individual phase. Moreover, the diffraction pattern is nearly invariant with milling time. This indicates that the milling does not lead to the formation of new phases.

The change of the average strain during the milling process coincides with the constant grain size value in the milled 49Fe-49Co-2V powders. Koch [22] studied the evolution of nanocrystalline structure in single phase materials by mechanical attrition and concluded that the total strain, rather than milling energy or ball-powder-ball collision frequency, is responsible for determining the grain size of nanocrystalline. The strain value is almost constant through 20 to 60 hours of milling. This is thought to be responsible for the stable grain size value in the samples.

The influence of milling on the phase transformations in the powders on annealing was examined by thermal analysis. Fig. 10a and b show DTA and DSC curves of the as-received and milled powders. Upon heating, the 550°C anomaly, $\alpha' \rightarrow \alpha$, and $\alpha \rightarrow \gamma$ transformations are observed in the as-received and milled powders. The transition from $\alpha' \rightarrow \alpha$ suggests the presence of α' phase in the as-received and milled powder, though α' phase can not be identified by XRD and TEM. The temperatures, at which exothermic and endothermic peaks are observed, are listed in Table II. The peak temperatures listed in Table II were measured at the heating rates of 10 K/min for DTA and 20 K/min for DSC testing, respectively.

The 550°C anomaly of the as-received powder occurs at 542°C. As milling time increases, the temperatures of the 550°C anomaly decrease. It is evident that the milling enhances the anomaly of 49Fe-49Co-2V

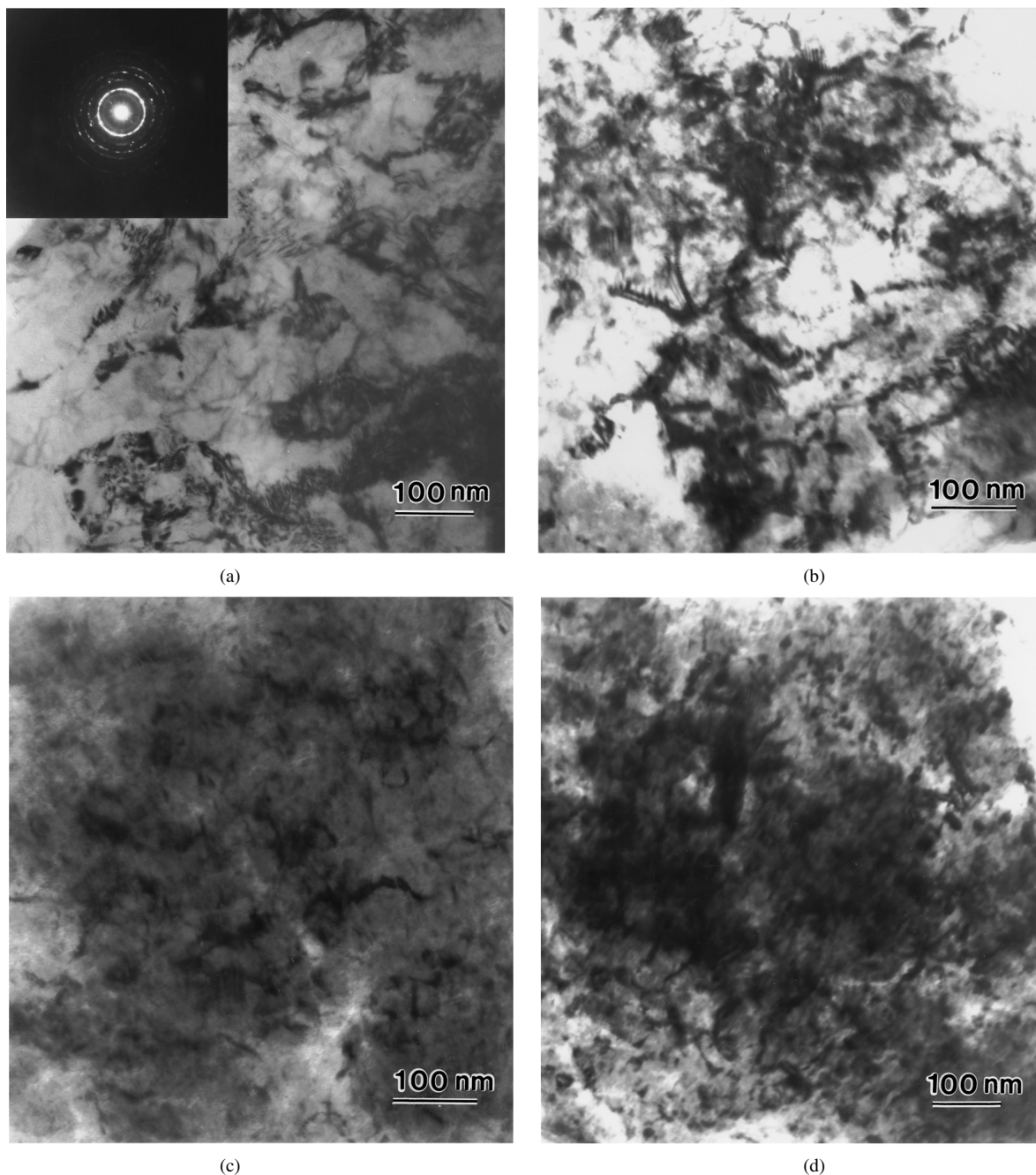


Figure 9 TEM bright field images of 49Fe-49Co-2V powders milled for different times, diffraction rings are {110}, {200}, {211}, {220} and {310} in order from inside to outside. (a) The as-received powder; (b) The powder milled for 20 hours; (c) the powder milled for 48 hours; (d) The powder milled for 60 hours.

TABLE II Peak temperatures in DTA and DSC curves of 49Fe-49Co-2V powders ($^{\circ}\text{C}$)

Milling time (hour)	550 $^{\circ}\text{C}$ anomaly	$\alpha' \rightarrow \alpha$	$\alpha \rightarrow \gamma$
0	542	729	944
8	526	729	944
20	522	729	944
36	517	729	944
48	519	730	973

powder. In the Fe-Co-V system, it was widely reported that martensite formed when the fcc γ phase was quickly cooled [11, 18, 23, 24]. When cooling rate reached approximately 100 $^{\circ}\text{C}/\text{sec}$, martensite, with either needle or plate form metallographical morphology and the same crystal structure and lattice parameter as

those of α , began to form at 500 $^{\circ}\text{C}$ [11]. Martensite transformation temperature varied only slightly with the cooling rate. Conversely, the temperature at which martensite began to transform reversely to the equilibrium phase, rose sensitively with increasing heating rate [11]. It is possible that martensite formed during the manufacturing process of the as-received powder. During mechanical milling, a high density of the deformed faults were introduced into the powder. Therefore, as the milling time increases, the temperature, at which the martensite reverse transformation occurs, decreases.

During heating, the $\alpha' \rightarrow \alpha$, and $\alpha \rightarrow \gamma$ transformations are both endothermic reactions. The influence of the milling on the transformation of $\alpha' \rightarrow \alpha$ is not observed. Milling up to 36 hours also does not affect

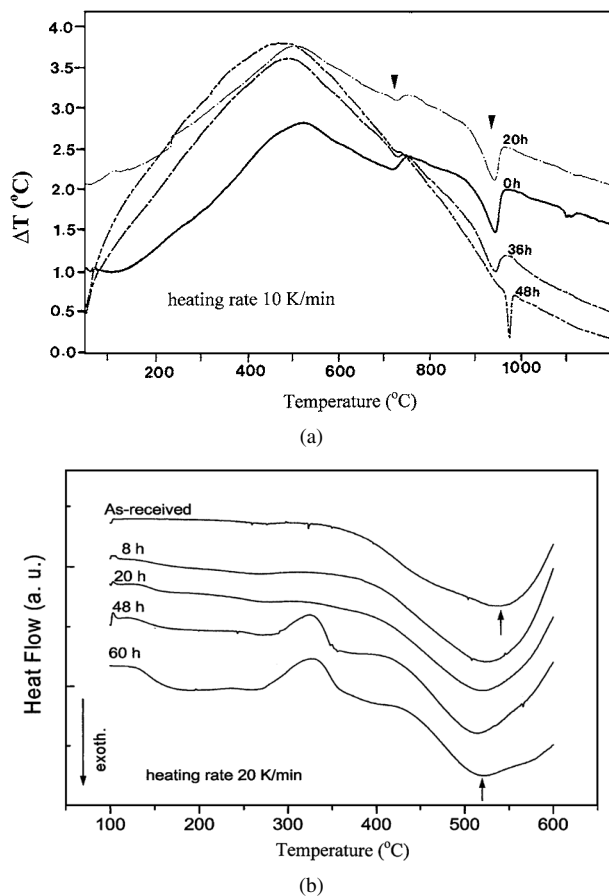


Figure 10 DTA and DSC curves of the as-received and milled 49Fe-49Co-2V powders. (a) DTA curves with a heating rate of 10 K/min. (b) DSC curves with a heating rate of 20 K/min.

the transformation of $\alpha \rightarrow \gamma$. However, in the powders milled for 48 hours, the $\alpha \rightarrow \gamma$ transformation is noticeably retarded by the milling.

Activation energy is one of the important parameters describing characteristics of phase transformation. The Kissinger equation is usually employed for determination of activation energy, which is expressed as [25]:

$$\frac{d\left[\ln\left(\frac{\phi}{T^2}\right)\right]}{d\left(\frac{1}{T}\right)} = -\frac{E}{R} \quad (2)$$

where ϕ is the heating rate, k/min.; T is characteristic temperature, in Kelvin degree. R is gas constant and E is activation energy. By plotting $\ln\left(\frac{\phi}{T^2}\right)$ against $\frac{1}{T}$, the value of E can be derived from the slope of the straight line plotted. Using the Kissinger equation, the values of activation energy for both as-received and milled powders were calculated and the results are listed in Table III. The results also indicate that milling promotes 550°C anomaly and does not affect transformation temperatures of $\alpha' \rightarrow \alpha$ and $\alpha \rightarrow \gamma$.

TABLE III Influence of milling on activation energy of phase transformation (KJ/mol)

Milling time (h)	550°C anomaly	$\alpha' \rightarrow \alpha$	$\alpha \rightarrow \gamma$
0	198 ± 10	626 ± 30	1531 ± 75
20		621 ± 30	1527 ± 75
48	184 ± 10		

Koch [26] systematically discussed structural changes caused by mechanical milling. Heavy plastic deformation (>20%) can destroy long range chemical order in ordered alloys [27]. The complete disordering by milling of the ordered Ni₃Al intermetallic compound was observed by Jang and Koch [28]. While in milled AlRu [29] and CuTi₂ [30] intermetallic compounds which were completely ordered, particularly saturated values of long-range order parameter for individual alloy systems were retained. This indicates that the milling decreases the ordering, however, the extent of disordering due to milling is a function of alloy chemistry. In reference to the present alloy, the decrease in degree of long range order due to milling is equivalent to an increase in the ductility of the alloy. The SEM observation of flaky and pallet particles at longer milling times is thought to be evidence for the improved ductility of the alloy.

4. Conclusions

Commercially available 49Fe-49Co-2V pre-alloyed powder was immersed in Methanol and mechanically milled up to 60 hours. The results obtained are summarized as follows.

1. The milling introduced severe plastic deformation in the powders, resulting in flaky and disk-like particles from spherical powders. Approximately 440% plastic deformation occurred after 60 hours of millings. However, the average volume of the particles was nearly constant at around 7100 μm^3 . The particle size and morphological changes on milling suggested the improved ductility of the alloy at longer milling. The mixing, caused by overlapping, cold welding and fracturing, among particles did not play an important role in the milling of 49Fe-49Co-2V powder.
2. Formation of nanocrystalline with an average grain size of approximately 35 nm can be achieved by milling of 20 hours. On further milling, the average grain size kept essentially constant. The average strain was found to be almost constant through 20 to 60 hours of milling.
3. The mechanical milling did not lead to the formation of new phases in the milled 49Fe-49Co-2V powders. However, the milling enhanced the 550°C anomaly.

Acknowledgement

The authors would like to acknowledge financial support provided by Printronix Inc. and the Office of Naval Research (Grants No.: N00014-94-1-0017, N00014-98-1-0569 and N00014-00-1-0109).

References

1. L. LI, *J. Appl. Phys* **79** (1996) 4578.
2. Z. TURGUT, J. H. SCOTT, M. Q. HUANG, S. A. MAJETICH and M. E. MCHENRY, *ibid.* **83** (1998) 6468.

3. T. NISHIZAWA and K. ISHIDA, in "Binary Alloy Phase Diagrams" edited by T. B. Massalski, 2nd ed. (Materials Park, Ohio, ASM International, 1990) p. 1187.
4. *Idem.*, *Bull. Alloy Phase Diagrams* **5** (1984) 250.
5. T. YOKOYAMA, T. TAKEZAWA and Y. HIGASHIDA, *Trans. JIM* **2** (1971) 30.
6. V. I. GOMAN'KOV, D. P. LITVIN, A. A. LOSHMANOV, B. G. LYASHCHENKO and I. M. PUZEI, *Sov. Phys. Crystallogr.* **7** (1962) 637.
7. C. SURYANARAYANA, *Inter. Mater. Rev.* **40** (1995) 41.
8. K. SUZUKI, in "Mater. Sci. Forum" (Vol. 312–314) edited by A. Calka and D. Wexler (Trans Tech Publications, Switzerland, 1999) p. 521.
9. G. HERZER, *Scripta Metall. Mater.* **33** (1995) 1741.
10. Z. TURGUT, M. Q. HUANG, K. GALLAGHER and M. E. MCHENRY, *J. Appl. Phys.* **81** (1997) 4039.
11. C. W. CHEN, *ibid.* **32** (1961) 348.
12. R. ELKALKOULI, M. GROSBRAS and J. F. DINHUT, *Nanostructured Mater.* **5** (1995) 733.
13. M. L. LAU, H. G. JIANG, W. NUCHFER and E. J. LAVERNIA, *Phys. Stat. Sol. (a)* **166** (1998) 257.
14. J. HE, M. ICE and E. J. LAVERNIA, *Nanostructured Mater.* **10** (1998) 1271.
15. J. HE, M. ICE, S. DALLEK and E. J. LAVERNIA, *Met. & Mat. Trans A* **31A** (2000) 541.
16. J. HE, M. ICE and E. J. LAVERNIA, *ibid.* **31A** (2000) 555.
17. J. A. OYEDELE and M. F. COLLINS, *Phys. Rev. B* **16** (1977) 3208.
18. P. M. NOVOTNY, *J. Appl. Phys.* **63** (1988) 2977.
19. M. W. BRANSON, R. V. MAJOR, C. PITT and R. D. RAWLINGS, *J. Magnetism and Magnetic Materials* **19** (1980) 222.
20. H. P. KLUG and L. E. ALEXANDER, in "X-ray Diffraction Procedures" (Wiley & Sons. Inc., New York, 1966) p. 138.
21. J. W. JEFFERY, in "Methods in X-Ray Crystallography" (Academic Press, London and New York, 1971) p. 86.
22. C. C. KOCH, *Nanostructured Mater.* **9** (1997) 13.
23. G. V. RAYNOR and V. G. RIVLIN, *Inter. Met. Rev.* **28** (1983) 211.
24. J. A. ASHBY, H. M. FLOWER and R. D. RAWLINGS, *Met. Sci.* **11** (1977) 91.
25. H. E. KISSINGER, *Anal. Chem.* **29** (1957) 1702.
26. C. C. KOCH, in "Mater. Sci. Forum," edited by P. H. Shingu, Vol. 88–89 (Trans Tech Publications, Switzerland, 1992) p. 243.
27. N. S. STOLOFF and R. G. DAVIES, *Progress in Materials Science* **13** (1966) 77.
28. J. S. C. JANG and C. C. KOCH, *J. Mater. Res.* **5** (1990) 498.
29. E. HELLSTERN, H. J. FECHT, Z. FU and W. L. JOHNSON, *J. Appl. Phys.* **65** (1989) 305.
30. Y. SEKI and W. L. JOHNSON, in "Solid-State Processing" edited by A. H. Clauer and J. J. de Barbadillo (TMS, Warrendale, PA, 1990) p. 287.

*Received 24 April
and accepted 13 November 2000*